Genetic Heterogeneity in Cellular Angiofibromas

Ioannis Panagopoulos[1] | Kristin Andersen[1] | Ingvild Lobmaier[2] | Marius Lund-Iversen[2]

[1]Section for Cancer Cytogenetics, Institute for Cancer Genetics and Informatics, The Norwegian Radium Hospital, Oslo University Hospital, Oslo, Norway | [2]Department of Pathology, The Norwegian Radium Hospital, Oslo University Hospital, Oslo, Norway

Correspondence: Ioannis Panagopoulos (ioapan@ous-hf.no)

ABSTRACT

Background: Cellular angiofibroma, a rare benign mesenchymal neoplasm, is classified within the 13q/RB1 family of tumors due to morphological, immunohistochemical, and genetic similarities with spindle cell lipoma. Here, genetic data reveal pathogenetic heterogeneity in cellular angiofibroma.

Methods: Three cellular angiofibromas were studied using G-banding/Karyotyping, array comparative genomic hybridization, RNA sequencing, and direct cycling sequencing.

Results: The first tumor carried a del(13)(q12) together with heterozygous loss and minimal expression of the *RB1* gene. Tumors two and three displayed chromosome 8 abnormalities associated with chimeras of the pleomorphic adenoma gene 1 (*PLAG1*). In tumor 2, the cathepsin B (*CTSB*) fused to *PLAG1* (*CTSB::PLAG1*) while in tumor 3, the mir-99a-let-7c cluster host gene (*MIR99AHG*) fused to *PLAG1* (*MIR99AHG::PLAG1*), both leading to elevated expression of *PLAG1* and insulin growth factor 2.

Conclusion: This study uncovers two genetic pathways contributing to the pathogenetic heterogeneity within cellular angiofibromas. The first aligns with the 13q/RB1 family of tumors and the second involves *PLAG1*-chimeras. These findings highlight the diverse genetic landscape of cellular angiofibromas, providing insights into potential diagnostic strategies.

1 | Introduction

Cellular angiofibroma is a rare benign mesenchymal neoplasm typically located in the superficial soft tissues of the vulva, as well as the inguinoscrotal or paratesticular region [1–5]. Its occurrence in other regions is even less common [3, 6–10].

The cytogenetic information of cellular angiofibroma, limited to only three cases, revealed involvement of chromosome 13 with loss of 13q [11–13]. Deletions of the *RB1* and *FOXO1* loci, located on chromosome band 13q14, were also found with interphase fluorescence in situ hybridization (FISH) [4, 8, 14, 15]. Because of morphological, immunohistochemical, and genetic similarities with spindle cell lipoma and myofibroblastoma, cellular

angiofibroma has been suggested to belong to the so-called 13q/RB1 family of tumors [4, 12, 16–20].

Here, we present the cytogenetic and molecular genetic findings of three cases of cellular angiofibroma, revealing pathogenetic heterogeneity in these tumors.

2 | Materials and Methods

2.1 | Patients

Table 1 provides information on the patients' gender and age, tumor locations and sizes, brief descriptions of the tumors, immunohistochemistry results, karyotype (G-banding), and

TABLE 1 | Clinicopathological and genetic data of the three studied cases.

Case	Gender/age (years)	Location	Size (cm)	Description	Immunohistochemistry	Karyotype	Molecular genetic data
1	Male/49	Perineum	7×5×3.5	Well-circumscribed, fibrous tumor with spindle cells without atypia, scattered fat cells within the tumor, scattered vessels, partly thick-walled, and partly hyalinized.	CD34+, AR+, ER+	46,Y,-X,?del(2)(q33),del(13)(q12),+r[2]	Deletion of the *RB1* and *FOXO1* genes
2	Female/41	Retroperitoneum	19.5×13.5×11.5	Well-circumscribed, fibrous, and myxoid tumor, partly paucicellular, partly more fibrous with spindle cells without atypia, scattered fat cells within the tumor, scattered vessels, partly thick-walled, and partly hyalinized.	CD34−, ACTA2+, DES+, ER+, PGR+	47~48,XX,+8,der(8)(8qter->8q21::?->cen->?::8q13->8qter)x2,+mar[cp14]	*CTSB::PLAG1* chimera
3	Female/48	Abdominal wall	10.5×6.8×4.1	Well-circumscribed, fibrous and myxoid tumor, paucicellular with spindle cells without atypia, scattered fat cells within the tumor, scattered vessels, and partly thick-walled.	CD34−/+, ACTA2-, ER+, PGR+, AR+, DES+, RB1 partially retained	45,XX,der(3)t(3;8)(q12;q13),dic(8;21)(q11~12;q21),der(20)t(20;21)(p11;q21)[12]	*MIR99AHG::PLAG1* chimera

Abbreviations: −, negative; +, positive; ACTA2, actin alpha 2, smooth muscle; AR, Androgen receptor; CD34, CD34 molecule; DES, desmin; ER, estrogen receptor; PGR, progesterone receptor; RB1, RB transcriptional corepressor 1.
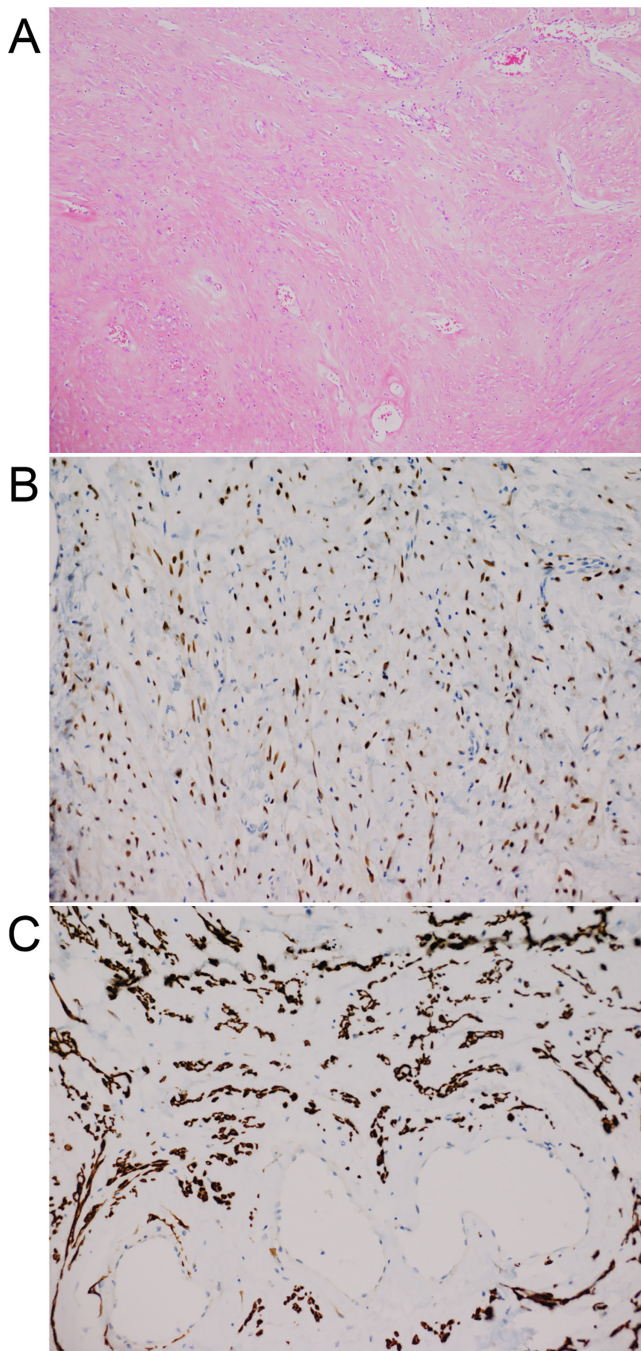
FIGURE 1 | Microscopic examination of the tumor from Case 2. (A) Hematoxylin and eosin-stained section at 100× magnification. (B) Immunohistochemical staining showing expression of estrogen receptor at 200× magnification. (C) Immunohistochemical staining showing expression of desmin at 200× magnification.

molecular genetic data. Figures 1 and 2 illustrate the microscopic examinations of Cases 2 and 3, respectively. The study was approved by the Regional committees for medical and health research ethics (REK) (https://www.forskningsetikk.no/en/). All patient information has been de-identified.
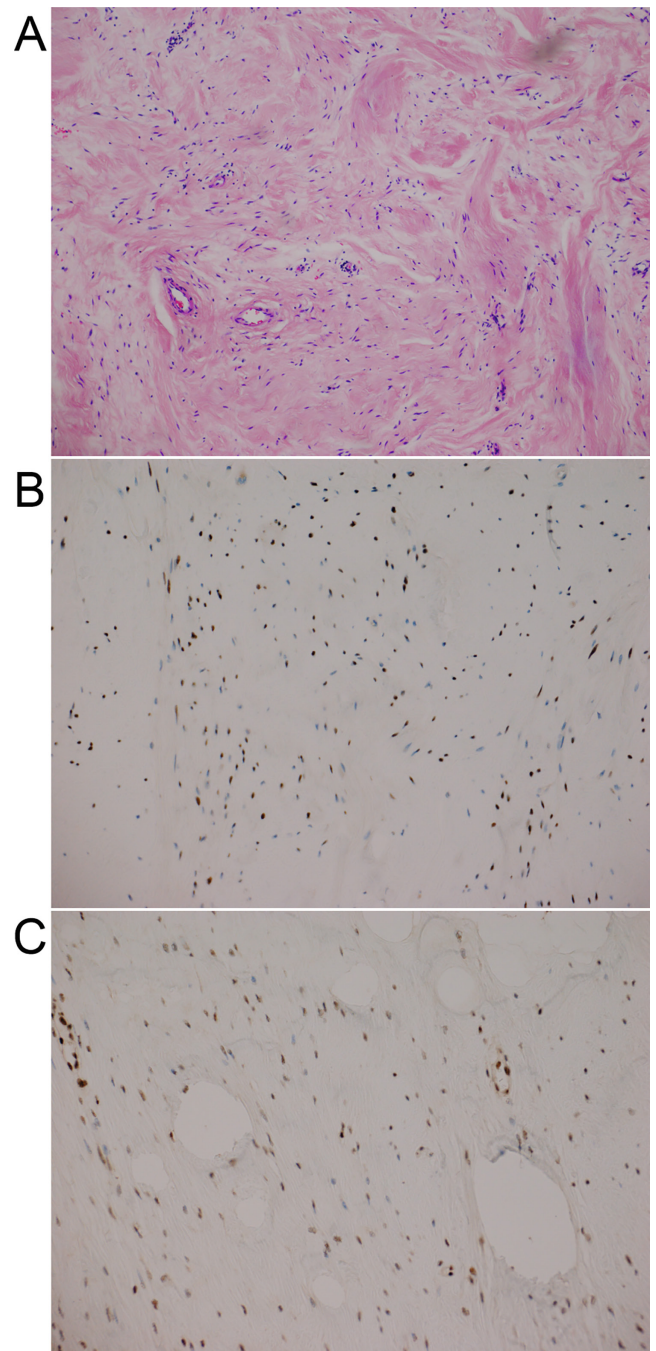
FIGURE 2 | Microscopic examination of the tumor from Case 3. (A) Hematoxylin and eosin-stained section at 100× magnification. (B) Immunohistochemical staining showing expression of estrogen receptor at 200× magnification. (C) Immunohistochemical staining showing expression of RB1 at 200× magnification.

2.2 | Methods

The methods we used in the present study had been described in details in many of our previous studies [12, 19–24]. A brief description of each method is given here.

TABLE 2 | Designation, sequence (5′→3′), and position in reference sequences of the forward (F1) and reverse (R1) primers used for direct sequencing, that is, polymerase chain reaction amplification and Sanger sequencing analyses.

Designation: Sequence (5′→3′)	Reference sequence: Position
CTSB-30F1: AACGCCAACCGCTCCGCT	NM_001908.5: 30–47
PLAG1-458R1: TTGTTGGACACTTGGGAACTGCC	NM_002655.2: 480–458
NR_136542-415F1: GCCCAACCAGTTCTTCATCTGGA	NR_136542.1: 415–437
NR_136542-437F1: AGACAGTTCAACGTTCTGCAAACCA	NR_136542.1: 437–461
NR_136545-420F1: TGTGGAAGGTAGCCTGTTACAGTGC	NR_136545.1: 420–444
NR_136545-445F1: TGGATTCATAAAAGGGCCTTTATGG	NR_136545.1: 445–469
PLAG1-352R1: TGATGGAAAAAGCCTCAGACTTTGA	NM_002655.2: 352–376
PLAG1-405R1: GGCTTCTCAAGTTTCATGTGGTCG	NM_002655.2: 428–405

Note: The forward primers had the M13 forward primer sequence TGTAAAACGACGGCCAGT at their 5′-end. The reverse primers had the M13 reverse primer sequence CAGGAAACAGCTATGACC at their 5′-end.

Abbreviations: CTSB, cathepsin B; NR_136542.1, transcript variant 6 of the mir-99a-let-7c cluster host gene; NR_136545.1, transcript variant 9 of the mir-99a-let-7c cluster host gene; PLAG1, pleomorphic adenoma gene 1 zinc finger.
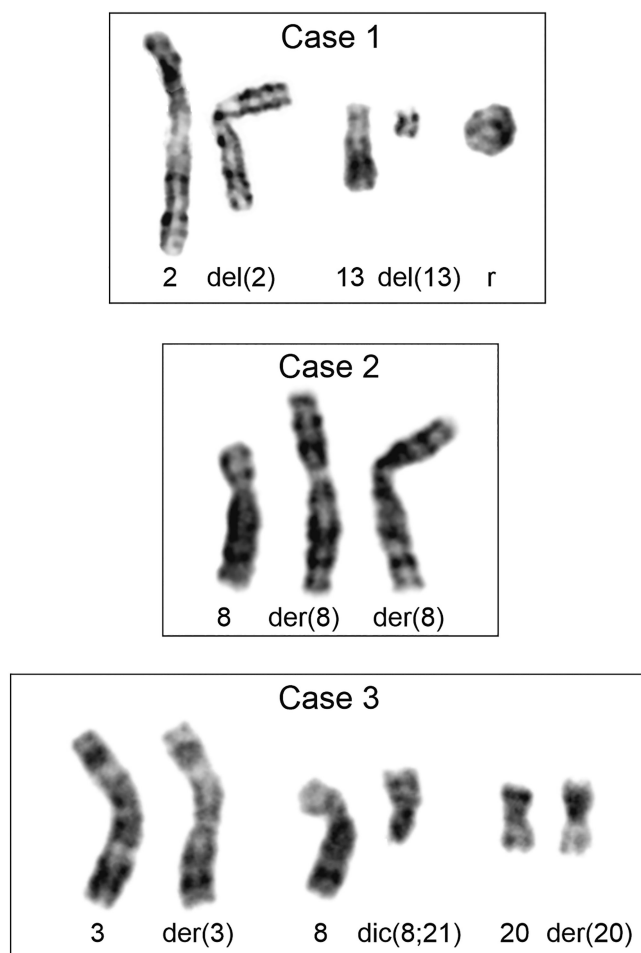
FIGURE 3 | Cytogenetic analysis of the three cellular angiofibromas. Partial karyotypes showing the aberrant chromosomes together with the corresponding normal chromosome homologs. For Case 1, del(2)(q33), del(13)(q12), and ring chromosome (r) together with chromosomes 2 and 13 are shown. For Case 2, the two der(8)(8qter->8q21::?->cen->?::8q13->8qter) together with chromosome 8 are shown. For Case 3, der(3)t(3;8)(q12; q13), dic(8;21)(q11–12;q21), and der(20)t(20;21)(p11;q21) together with chromosomes 3, 8, and 20 are shown.

2.3 | G-Banding and Karyotyping

Fresh tissue from a representative area of the tumors was minced with scalpels into 1–2 mm fragments and then subjected to enzymatic disaggregation using collagenase II (Worthington, Freehold, NJ, USA). Subsequently, the resulting cells were cultured, harvested, and processed for cytogenetic examination using established techniques [25, 26]. Chromosome preparations were G-banded with Wright's stain (Sigma-Aldrich; St Louis, MO, USA) and examined [25, 26]. The karyotypes were described in accordance with the International System for Human Cytogenomic Nomenclature [27].

2.4 | DNA and RNA Isolation

Genomic DNA and total RNA were extracted from tumor tissue adjacent to that used for cytogenetic analysis and histologic examination. The tissue had been frozen and stored at −80°C. Genomic DNA was extracted using the Maxwell 16 Instrument System and Maxwell 16 Cell DNA Purification Kit (Promega, Madison, Wisconsin, USA) and the concentration was measured using a Quantus fluorometer (Promega). Total RNA was extracted using the miRNeasy Mini Kit and QiaCube automated purification system according to the manufacturer's instructions (Qiagen, Hilden, Germany), and the concentration was measured with the QIAxpert microfluidic UV/VIS spectrophotometer (Qiagen). The Agilent 2100 bioanalyzer and the DV200 index, which evaluates the percentage of RNA that is longer than 200 nucleotides, were used to assess RNA integrity [28].

2.5 | Array Comparative Genomic Hybridization Analysis

Array comparative genomic hybridization (aCGH) was conducted utilizing the CytoSure array products (Oxford Gene Technology, Begbroke, Oxfordshire, UK) following the protocols
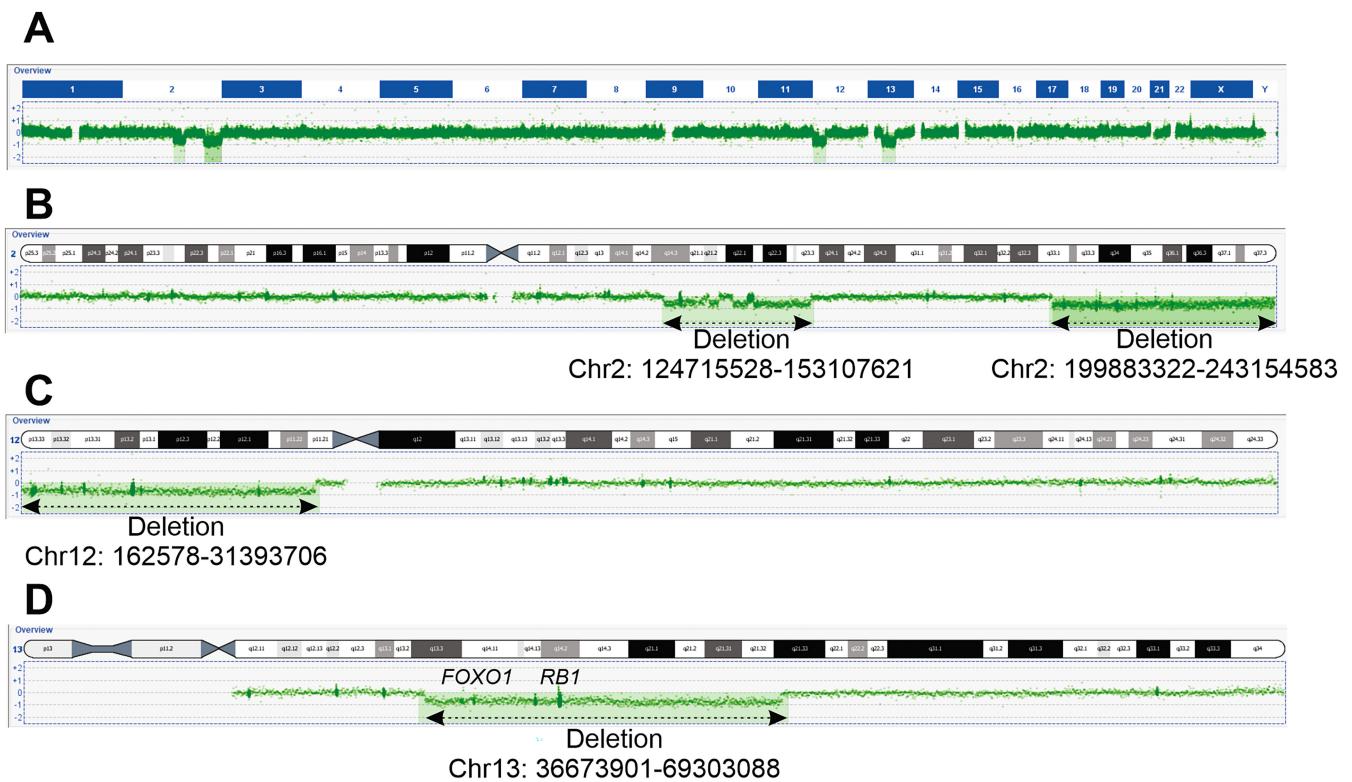
FIGURE 4 | Array comparative genomic hybridization (aCGH) examination of the tumor from Case 1. (A) Genetic profile of whole genome showing losses from parts of chromosomes 2, 12, and 13. (B) aCGH showing the deleted parts of the q arm of chromosome 2. (C) aCGH showing the deleted part of the p arm of chromosome 12. (D) aCGH showing the deleted part of the q arm of chromosome 13. The positions of the *FOXO1* and *RB1* genes are also shown.

provided by the company [21, 22]. Promega's human genomic DNA served as the reference DNA (Promega). The slides (CytoSure Cancer +SNP array 4x180k) were scanned in an Agilent SureScan Dx microarray scanner using Agilent Feature Extraction Software (version 12.1.1.1). Data were analyzed using the CytoSure Interpret analysis software (version 4.11.36). The software annotations are based on human genome build 19.

2.6 | RNA Sequencing

High-throughput paired-end RNA-sequencing was performed at the Genomics Core Facility, Norwegian Radium Hospital, Oslo University Hospital. The software FusionCatcher was used to find chimeric transcripts [29, 30]. For quantification and differential analysis of RNA sequencing data (expression analysis), the program Kallisto was used, respectively [31]. Quantification was calculated as transcripts per million (TPM) which is a measurement of the proportion of transcripts in the pool of RNA [31]. Expression analysis was based on Ensembl release 95 (January 2019). Transcripts from the following genes were quantified: Collagen type I alpha 2 chain (*COL1A2* on 7q21.3), collagen type I alpha 1 chain (*COL1A1* on 17q21.33), collagen type III alpha 1 chain (*COL3A1* on 2q32.2), RB transcriptional corepressor 1 (*RB1* located on chromosomal subband 13q14.2), pleomorphic adenoma gene 1 (*PLAG1* on 8q12.1), and insulin like growth factor 2 (*IGF2* on11p15.5).

2.7 | Reverse Transcription-Polymerase Chain Reaction and Sanger Sequencing Analyses

The primers used for polymerase chain reaction (PCR) amplifications are shown in Table 2. Reverse transcription (RT-PCR) and Sanger sequencing analyses were performed using the Direct Cycle Sequencing Kit according to the company's recommendations (ThermoFisher Scientific, Waltham, MA, USA). The methodologies for cDNA synthesis, RT-PCR amplification, and Sanger sequencing are described elsewhere [21–24]. The following primer combinations were used: CTSB-30F1/PLAG1-458R1 for Sample 2, NR_136542-415F1/PLAG1-405R1, NR_136542-437F1/PLAG1-352R1, NR_136545-420F1/ PLAG1-405R1, and NR_136545-445F1/ PLAG1-352R1 for Sample 3. The forward primers (F1) had the M13 forward primer sequence TGTAAAACGACGGCCAGT at their 5′-end. The reverse primers (R1) had the M13 reverse primer sequence CAGGAAACAGCTATGACC at their 5′-end.

The basic local alignment search tool (BLAST) [32] was used to compare the sequences, which were obtained by Sanger sequencing, with the following NCBI reference sequences: for Sample 2, NM_001908.5 corresponding to cathepsin B (*CTSB*), transcript variant 1, and NM_002655.2 for transcript variant 1of pleomorphic adenoma gene 1 (*PLAG1*). For Sample 3, NR_136545.1, corresponding to transcript variant 9 of mir-99a-let-7c cluster host gene (*MIR99AHG*), NR_136542.1, corresponding to transcript variant 6 of *MIR99AHG*, and NM_002655.2 of *PLAG1*. The sequences

TABLE 3 | Fusion transcripts detected in four cases of cellular angiofibroma after analysis of RNA sequencing data with FusionCatcher.

Case	Fusion transcript	Fusion sequence
1	Not done	—
2	CTSB::PLAG1 (Exon 1–Exon 3)	GCTGCGCGCAGGCTGGGCTGCAGGCTCTCGGCTGCAGCGCTGG::ATTGGCCAAAATGGGAAGGATTGGATTCCACTCTTCCACGA
3	MIR99AHG::PLAG1 NR_136545.1::PLAG1 (Exon 1–Exon 3)	GGAGGAAACTTTTTGATCTGCAGAAAAGCCAGAAGACATCTAG::ATTGGCCAAAATGGGAAGGATTGGATTCCACTCTTCCACGA
3	MIR99AHG::PLAG1 NR_136542::PLAG1 (Exon 5–Exon 3)	AATGTCAAGATTTGAACAAGAAGAGAATGGAATACACAATATG::ATTGGCCAAAATGGGAAGGATTGGATTCCACTCTTCCACGA

were also aligned on the Human GRCh37/hg19 assembly using the BLAST-like alignment tool (BLAT) and the human genome browser hosted by the University of California, Santa Cruz [33, 34].

3 | Results

3.1 | Karyotyping and aCGH Analyses

All tumors had cells carrying clonal chromosomal aberrations (Table 1). The abnormal karyotypes were pseudo- or near-diploid and involved either losses of material from chromosome 13 (Case 1) or structural aberrations encompassing chromosome bands 8q11–q13 (Cases 2 and 3). Notably, no two tumors shared identical karyotypes (Table 1; Figure 3).

Case 1 had abnormal karyotype containing heterozygous loss of material from the chromosome 13 together with other chromosome aberrations (Table 1). There was a deletion in chromosome 13, described as del(13)(q12), together with a deletion in chromosome, del(2)(q33), and a ring chromosome (Table 1; Figure 3).

Cases 2 and 3 displayed abnormal karyotypes with aberrations involving chromosome 8 (Table 1; Figure 3). In Case 2, a composite karyotype containing clonally occurring aberrations, had an extra chromosome 8, two copies of a derivative chromosome 8 generated by rearrangements within chromosome 8, and a marker chromosome. In Case 3, the abnormal karyotype included a structurally rearranged chromosome generated by chromosome bands 3q12 and 8q13 described as der(3)t(3;8)(q12;q13), a dicentric chromosome with breaks and reunion at bands 8 q11–12 and 21q21, dic(8;21)(q11–12;q21), and a structurally rearranged chromosome generated by chromosome bands 20p11 and 21q21 described as der(20)t(20;21)(p11;q21) (Table 1; Figure 3).

aCGH analysis was performed on Case 1. No material was available for the other two cases precluding aCGH examination. In Case 1, aCGH revealed no loss of chromosome X, confirmed the presence of del(2)(q33), revealed an interstitial deletion on chromosome 2 from 2q14,3 to 2q23.3, and uncovered an interstitial deletion on chromosome 13 from 13q13.3 to13q21.33, encompassing the *RB1* and *FOXO1* genes. Additionally, a deletion on the p arm of chromosome 12 from 12p13.33 to 12.p11.21 was detected (Figure 4).

3.2 | Detection of Chimeras

Because the tumor in Case 1 had a cytogenetically profile typical of cellular angiofibroma, characterized by the loss of material from chromosome 13, including *RB1* (Table 1 and Figure 1), a search for chimeric transcripts was not conducted on the raw RNA sequencing data of this case.

In tumor 2, the analysis of raw RNA sequencing data with FusionCatcher detected a chimeric transcript between the noncoding exon 1 of *CTSB* from 8p23.1 and the noncoding exon 3 of *PLAG1* from 8q12.1 (*CTSB::PLAG1* chimeric transcript Table 3). Direct cycle sequencing using the primer combination
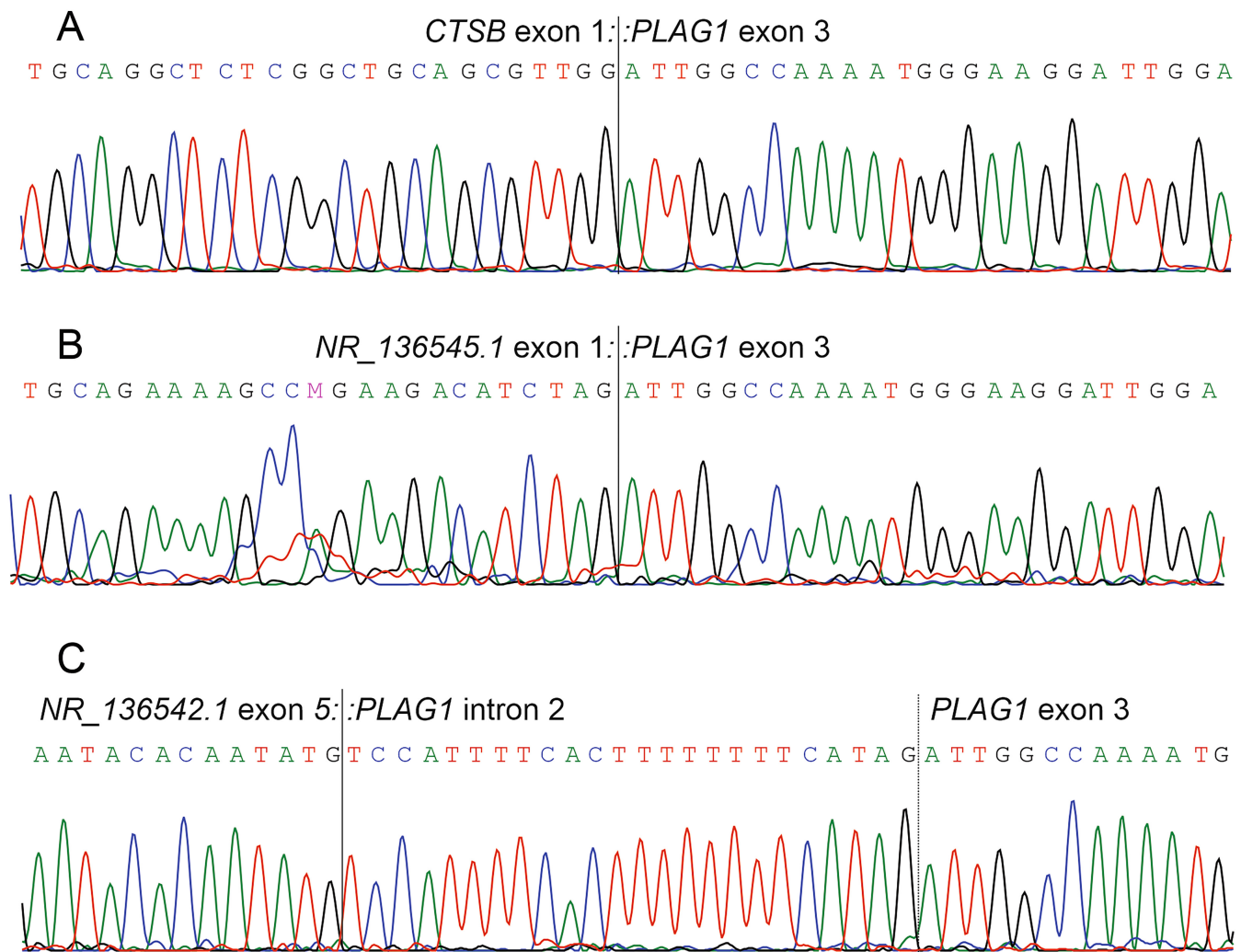
FIGURE 5 | Direct cycle sequencing results showing the *PLAG1*-chimeras found in cellular angiofibroma of Cases 3 and 4. (A) Partial sequence chromatogram showing the junction between exon 1 of cathepsin B (*CTSB*) and exon 3 of pleomorphic adenoma 1 (*PLAG1*) genes, which was found in Case 3. The exon numbers were based on the sequences with accession numbers NM_001908.5 and NM_002655.2 corresponding to transcript variant 1 of *CTSB* and transcript variant 1 of *PLAG1*, respectively. (B) and (C) Partial sequence chromatograms showing the junctions between mir-99a-let-7c cluster host gene (*MIR99AHG*) and *PLAG1*, which were found in Case 4. (B) The junction between exon 1 of the reference sequence NR_136545.1, corresponding to transcript variant 9 of *MIR99AHG*, and exon 3 of *PLAG1*. (C) The junction between exon 5 of the reference sequence NR_136542.1, corresponding to transcript variant 6 of *MIR99AHG*, and intron 2 of *PLAG1*, 24 nucleotides upstream of exon 3 of *PLAG1*.

CTSB-30F1/PLAG1-458R1 confirmed the presence of the *CTSB::PLAG1* chimeric transcript (Table 3; Figure 5A).

In tumor 3, two chimeric *MIR99AHG::PLAG1* transcripts were detected. In the first transcript, exon 1 of the reference sequence NR_136545.1 (corresponding to transcript variant 9 of *MIR99AHG*) fused to exon 3 of *PLAG1* (*NR_136545.1::PLAG1*, Table 3). In the second chimeric transcript, exon 5 of the reference sequence *NR_136542.1* (corresponding to transcript variant 6 of *MIR99AHG*) fused to exon 3 of *PLAG1* (*NR_136542.1::PLAG1*).

Direct cycle sequencing using the primer combination NR_136545-420F1/PLAG1-405R1, and NR_136545-445F1/PLAG1-352R1 confirmed the *NR_136545.1::PLAG1* chimeric transcript detected by FusionCatcher (Figure 5B). Sequencing with the primer combinations NR_136542-415F1/PLAG1-405R1, NR_136542-437F1/PLAG1-352R1 detected a transcript in which of exon 5 of *NR_136542.1* fused with an intronic sequence of *PLAG1*, 26 nucleotides upstream of exon 3 of the *PLAG1* gene (Figure 5C). No additional PCR/Sanger sequencing experiments were performed to detected the fusion of exon 5 from NR_136542.1 with exon 3 of *PLAG1* found by FusionCatcher.

3.3 | Expression Analysis

The results obtained with Kallisto program are shown in Table 4. High expression of *CO1A2*, *COL1A1*, and *COL3A1* were found in all three tumors. The *RB1* gene was expressed in tumors 2 and 3 while its expression was negligible in tumor 1, which carried the interstitial deletion on chromosome 13 encompassing *RB1* (Tables 1 and 4; Figures 3 and 4). In tumors 2 and 3, characterized by aberrations of chromosome 8 and carried *CTSB::PLAG1* (tumor 2) and *MIR99AHG::PLAG1* (tumor 3), high expression of

TABLE 4 | Expression analysis of the genes collagen type I alpha 2 chain (*COL1A2*), collagen type I alpha 1 chain (*COL1A1*), collagen type III alpha 1 chain (*COL3A1*), RB transcriptional corepressor 1 (*RB1*), pleiomorphic adenoma gene 1 (*PLAG1*), and insulin like growth factor 2 (*IGF2*).

Gene	Transcript	Expression (TPM)		
		Case 1	Case 2	Case 3
COL1A2	ENST00000620463.1	4871.95	4212.6	3717.3
COL1A1	ENST00000225964.9	3111.26	3310.54	3413.3
COL3A1	ENST00000304636.7	3013.28	2904.18	3040.69
RB1	ENST00000267163.5	0.18	32.02	17.47
	ENST00000643064.1	0.59	5.56	12.12
	ENST00000531171.5	0.38	3.70	4.53
	ENST00000467505.5	2.67	0.28	1.97
	ENST00000525036.1	0.40	0	0.36
	ENST00000646097.1	0	5.75	7.57
	ENST00000650461.1	0	2.14	2.91
	ENST00000484879.1	0	8.51	1.83
PLAG1	ENST00000423799.6	0.33	32.74	28.83
	ENST00000429357.2	0.0	30.81	28.35
IGF2	ENST00000418738.2	5.60	318.73	4101.84
	ENST00000381392.5	1.58	142.11	1018.23
	ENST00000381406.8	0.09	11.81	61.21
	ENST00000416167.7	0	15.81	141.49
	ENST00000434045.6	0	6.45	3.07
	ENST00000381389.5	0	2.24	5.38
	ENST00000381395.5	0	0.12	1.40

Note: Quantification was calculated as transcripts per million (TPM). Only the transcripts coding for protein are reported. Expression was based on Ensembl 96: April 2019.

PLAG1 was found. Expression of *PLAG1* was negligible in tumor 1 (Table 4). Additionally, the *IGF2* gene showed elevated expression in tumors 2 and 3 compared with tumor 1 (Table 4).

4 | Discussion

The present study delineates two distinct genetic pathways in cellular angiofibromas demonstrating pathogenetic heterogeneity within this tumor type. The first genetic pathway, observed in Case 1, aligns with the pathway previously reported in the 13q/RB1 family of tumors, which includes spindle cell/pleomorphic lipoma, atypical spindle cell/pleomorphic lipomatous tumor, myofibroblastoma, cellular angiofibroma, and acral fibromyxoma [11–13]. A combination of G-banding and aCGH techniques revealed an interstitial deletion on chromosome 13 from 13q13.3 to13q21.33 in the tumor of Case 1. This deletion resulted in a heterozygous loss of numerous genes, including *RB1* and *FOXO1*. Additionally, analysis with the Kallisto program applied to the RNA sequencing data indicated a lack of *RB1* (Table 4). Moreover, the loss of material of chromosome13 was found together with other acquired chromosome aberrations

(Table 1). This cytogenetic pattern is consistent with findings in cellular angiofibromas and spindle cell lipomas [11, 12, 19, 35].

The second pathogenetic pathway found in cellular angiofibromas was seen in Cases 2 and 3. It involves the generation of *PLAG1*-chimeras, similar to those reported in many other tumor types including pleomorphic adenomas [36], lipoblastomas [37], 8q11-13/*PLAG1*-rearranged lipomatous tumors [24], chondroid syringoma [21], uterine myxoid leiomyosarcoma [38, 39], pediatric fibromyxoid tumor [40, 41], carcinoma ex pleomorphic adenoma [42], acute myeloid leukemia [43, 44], myoepithelioma/myoepithelial carcinoma/mixed tumors [45, 46], angiofibroma of soft tissue [47], and other soft tissue tumors [48, 49]. In all reported *PLAG1*-chimeras the 5′-end non-coding region of *PLAG1* is replaced by the 5′-end non-coding region of the 5′-end fusion partner gene, and the expression of *PLAG1* is controlled by the promoter of 5′-end fusion partner gene. The result is an overexpression or ectopic activation of *PLAG1* leading to deregulation of *PLAG1*-target genes and tumor formation [50–56]. *PLAG1* codes for a transcription factor that binds a core sequence, GRGGC, and a G-cluster, RGGK, separated by seven random nucleotides and activates transcription [50]. The PLAG1 protein was shown

to bind promoter 3 of the insulin growth factor 2 (*IGF2*) resulting in overexpression of *IGF2* and upregulation of the IGF signaling pathway [50, 55, 57]. Our results are in agreement with the above-mentioned description. Indeed, in the tumor 3 carrying *CSTB::PLAG1* and tumor 4 with *MIR99AHG::PLAG1*, (Tables 1 and 3) the expression of both *PLAG1* and *IGF2* genes was much higher than the expression found in tumor 1 which did not have *PLAG1*-chimeras (Table 4).

In conclusion, our study reveals two distinct genetic pathways contributing to the pathogenetic heterogeneity within cellular angiofibromas. The first pathway aligns with the 13q/RB1 family of tumors resulting in the loss of RB1 gene and its expression. The second pathway involves the generation of *PLAG1*-chimeras, a phenomenon reported in various tumor types. These chimeras result in overexpression of *PLAG1*, deregulation of *PLAG1*-target genes, and promotion of tumor formation. Our findings underscore the diverse genetic landscape of cellular angiofibromas, providing insights into potential diagnostic strategies.

Conflicts of Interest

The authors declare no conflicts of interest.

Data Availability Statement

All available data are included in the manuscript and its figures.

References

1. M. R. Nucci, S. R. Granter, and C. D. Fletcher, "Cellular Angiofibroma: A Benign Neoplasm Distinct From Angiomyofibroblastoma and Spindle Cell Lipoma," *American Journal of Surgical Pathology* 21, no. 6 (1997): 636–644.

2. W. B. Laskin, J. F. Fetsch, and F. K. Mostofi, "Angiomyofibroblastomalike Tumor of the Male Genital Tract: Analysis of 11 Cases With Comparison to Female Angiomyofibroblastoma and Spindle Cell Lipoma," *American Journal of Surgical Pathology* 22, no. 1 (1998): 6–16.

3. Y. Iwasa and C. D. Fletcher, "Cellular Angiofibroma: Clinicopathologic and Immunohistochemical Analysis of 51 Cases," *American Journal of Surgical Pathology* 28, no. 11 (2004): 1426–1435.

4. U. Flucke, J. H. van Krieken, and T. Mentzel, "Cellular Angiofibroma: Analysis of 25 Cases Emphasizing Its Relationship to Spindle Cell Lipoma and Mammary-Type Myofibroblastoma," *Modern Pathology* 24, no. 1 (2011): 82–89.

5. V. D. Mandato, S. Santagni, A. Cavazza, L. Aguzzoli, M. Abrate, and G. B. La Sala, "Cellular Angiofibroma in Women: A Review of the Literature," *Diagnostic Pathology* 10 (2015): 114.

6. J. F. Val-Bernal, S. Rubio, M. F. Garijo, and M. C. Gonzalez-Vela, "Extragenital Subcutaneous Cellular Angiofibroma," *Acta Pathologica, Microbiologica, Et Immunologica Scandinavica* 115, no. 3 (2007): 254–258.

7. Y. Omori, H. Saeki, K. Ito, et al., "Extragenital Subcutaneous Cellular Angiofibroma of the Elbow," *Journal of the European Academy of Dermatology and Venereology* 28, no. 6 (2014): 828–830.

8. I. Wyn, M. Debiec-Rychter, B. Van Cleynenbreugel, and R. Sciot, "Cellular Angiofibroma of the Prostate: A Rare Tumor in an Unusual Location," *Case Reports in Pathology* 2014 (2014): 871530.

9. C. Perrin, G. E. Cannata, F. Pedeutour, B. Dadone-Montaudié, and D. Ambrosetti, "Cellular Angiofibroma: Case Report of a Unique Subungual Presentation," *Acta Dermato-Venereologica* 99, no. 10 (2019): 915–916.

10. J. Das and N. Das, "Cellular Angiofibroma of Orbit—A Rare Tumor at the Rarest Location," *Orbit* 41, no. 2 (2022): 245–249.

11. M. Hameed, K. Clarke, H. Z. Amer, K. Mahmet, and S. Aisner, "Cellular Angiofibroma Is Genetically Similar to Spindle Cell Lipoma: A Case Report," *Cancer Genetics and Cytogenetics* 177, no. 2 (2007): 131–134.

12. I. Panagopoulos, L. Gorunova, B. Bjerkehagen, K. Andersen, M. Lund-Iversen, and S. Heim, "Loss of Chromosome 13 Material in Cellular Angiofibromas Indicates Pathogenetic Similarity With Spindle Cell Lipomas," *Diagnostic Pathology* 12, no. 1 (2017): 17.

13. S. Libbrecht, J. Van Dorpe, and D. Creytens, "The Rapidly Expanding Group of RB1-Deleted Soft Tissue Tumors: An Updated Review," *Diagnostics* 11, no. 3 (2021): 430.

14. B. J. Chen, A. Marino-Enriquez, C. D. Fletcher, and J. L. Hornick, "Loss of Retinoblastoma Protein Expression in Spindle Cell/Pleomorphic Lipomas and Cytogenetically Related Tumors: An Immunohistochemical Study With Diagnostic Implications," *American Journal of Surgical Pathology* 36, no. 8 (2012): 1119–1128.

15. F. Maggiani, M. Debiec-Rychter, M. Vanbockrijck, and R. Sciot, "Cellular Angiofibroma: Another Mesenchymal Tumour With 13q14 Involvement, Suggesting a Link With Spindle Cell Lipoma and (Extra)-Mammary Myofibroblastoma," *Histopathology* 51, no. 3 (2007): 410–412.

16. G. Magro, A. Righi, L. Casorzo, et al., "Mammary and Vaginal Myofibroblastomas Are Genetically Related Lesions: Fluorescence In Situ Hybridization Analysis Shows Deletion of 13q14 Region," *Human Pathology* 43, no. 11 (2012): 1887–1893.

17. B. E. Howitt and C. D. Fletcher, "Mammary-Type Myofibroblastoma: Clinicopathologic Characterization in a Series of 143 Cases," *American Journal of Surgical Pathology* 40, no. 3 (2016): 361–367.

18. A. Agaimy, M. Michal, J. Giedl, L. Hadravsky, and M. Michal, "Superficial Acral Fibromyxoma: Clinicopathological, Immunohistochemical, and Molecular Study of 11 Cases Highlighting Frequent Rb1 Loss/Deletions," *Human Pathology* 60 (2017): 192–198.

19. I. Panagopoulos, L. Gorunova, M. Lund-Iversen, et al., "Cytogenetics of Spindle Cell/Pleomorphic Lipomas: Karyotyping and FISH Analysis of 31 Tumors," *Cancer Genomics & Proteomics* 15, no. 3 (2018): 193–200.

20. I. Panagopoulos, L. Gorunova, M. Lund-Iversen, and S. Heim, "Monosomy 13 in Mammary Myofibroblastoma," *Anticancer Research* 41, no. 8 (2021): 3747–3751.

21. I. Panagopoulos, L. Gorunova, K. Andersen, et al., *NDRG1-PLAG1* and *TRPS1-PLAG1* Fusion Genes in Chondroid Syringoma," *Cancer Genomics & Proteomics* 17, no. 3 (2020): 237–248.

22. I. Panagopoulos, K. Andersen, M. Brunetti, et al., "Genetic Pathways in Peritoneal Mesothelioma Tumorigenesis," *Cancer Genomics & Proteomics* 20, no. 4 (2023): 363–374.

23. I. Panagopoulos, K. Andersen, M. Brunetti, et al., "Pathogenetic Dichotomy in Angioleiomyoma," *Cancer Genomics & Proteomics* 20, no. 6 (2023): 556–566.

24. I. Panagopoulos, K. Andersen, L. Gorunova, et al., "Recurrent 8q11-13 Aberrations Leading to *PLAG1* Rearrangements, Including Novel Chimeras *HNRNPA2B1::PLAG1* and *SDCBP::PLAG1*, in Lipomatous Tumors," *Cancer Genomics & Proteomics* 20, no. 2 (2023): 171–181.

25. P. Polito, P. Dal Cin, M. Debiec-Rychter, and A. Hagemeijer, "Human Solid Tumors: Cytogenetic Techniques," *Methods in Molecular Biology* 220 (2003): 135–150.

26. R. Lukeis and M. Suter, "Cytogenetics of Solid Tumours," *Methods in Molecular Biology* 730 (2011): 173–187.

27. J. McGowan-Jordan, R. J. Hastings, and S. Moore, *ISCN 2020: An International System for Human Cytogenomic Nomenclature (2020)* (Basel: Karger, 2020).

28. T. Matsubara, J. Soh, M. Morita, et al., "DV200 Index for Assessing RNA Integrity in Next-Generation Sequencing," *BioMed Research International* 2020 (2020): 9349132.

29. S. Kangaspeska, S. Hultsch, H. Edgren, D. Nicorici, A. Murumagi, and O. Kallioniemi, "Reanalysis of RNA-Sequencing Data Reveals Several Additional Fusion Genes With Multiple Isoforms," *PLoS One* 7, no. 10 (2012): e48745.

30. D. Nicorici, H. Satalan, H. Edgren, et al., "FusionCatcher – A Tool for Finding Somatic Fusion Genes in Paired-End RNA-Sequencing Data," *bioRxiv* (2014).

31. N. L. Bray, H. Pimentel, P. Melsted, and L. Pachter, "Near-Optimal Probabilistic RNA-seq Quantification," *Nature Biotechnology* 34, no. 5 (2016): 525–527.

32. S. F. Altschul, W. Gish, W. Miller, E. W. Myers, and D. J. Lipman, "Basic Local Alignment Search Tool," *Journal of Molecular Biology* 215, no. 3 (1990): 403–410.

33. W. J. Kent, "BLAT—The BLAST-Like Alignment Tool," *Genome Research* 12, no. 4 (2002): 656–664.

34. W. J. Kent, C. W. Sugnet, T. S. Furey, et al., "The Human Genome Browser at UCSC," *Genome Research* 12, no. 6 (2002): 996–1006.

35. I. Panagopoulos, L. Gorunova, I. Lobmaier, H. K. Andersen, B. Bjerkehagen, and S. Heim, "Cytogenetic Analysis of a Pseudoangiomatous Pleomorphic/Spindle Cell Lipoma," *Anticancer Research* 37, no. 5 (2017): 2219–2223.

36. K. Kas, M. L. Voz, E. Röijer, et al., "Promoter Swapping Between the Genes for a Novel Zinc Finger Protein and Beta-Catenin in Pleiomorphic Adenomas With t(3;8)(p21;q12) Translocations," *Nature Genetics* 15, no. 2 (1997): 170–174.

37. M. K. Hibbard, H. P. Kozakewich, P. Dal Cin, et al., "*PLAG1* Fusion Oncogenes in Lipoblastoma," *Cancer Research* 60, no. 17 (2000): 4869–4872.

38. J. A. Arias-Stella, 3rd, R. Benayed, E. Oliva, et al., "Novel *PLAG1* Gene Rearrangement Distinguishes a Subset of Uterine Myxoid Leiomyosarcoma From Other Uterine Myxoid Mesenchymal Tumors," *American Journal of Surgical Pathology* 43, no. 3 (2019): 382–388.

39. S. A. Thiryayi, G. Turashvili, E. K. Latta, et al., "*PLAG1*-Rearrangment in a Uterine Leiomyosarcoma With Myxoid Stroma and Heterologous Differentiation," *Genes, Chromosomes & Cancer* 60, no. 10 (2021): 713–717.

40. C. T. Chung, C. R. Antonescu, B. C. Dickson, et al., "Pediatric Fibromyxoid Soft Tissue Tumor With *PLAG1* Fusion: A Novel Entity?" *Genes, Chromosomes & Cancer* 60, no. 4 (2021): 263–271.

41. S. Santisukwongchote, P. S. Thorner, T. Desudchit, et al., "Pediatric Fibromyxoid Tumor With *PLAG1* Fusion: An Emerging Entity With a Novel Intracranial Location," *Neuropathology* 42, no. 4 (2022): 315–322.

42. N. Katabi, R. Ghossein, A. Ho, et al., "Consistent *PLAG1* and *HMGA2* Abnormalities Distinguish Carcinoma Ex-Pleomorphic Adenoma From Its De Novo Counterparts," *Human Pathology* 46, no. 1 (2015): 26–33.

43. U. Aypar, J. Yao, D. M. Londono, et al., "Rare and Novel *RUNX1* Fusions in Myeloid Neoplasms: A Single-Institute Experience," *Genes, Chromosomes & Cancer* 60, no. 2 (2021): 100–107.

44. P. Kerbs, S. Vosberg, S. Krebs, et al., "Fusion Gene Detection by RNA-Sequencing Complements Diagnostics of Acute Myeloid Leukemia and Identifies Recurring *NRIP1-MIR99AHG* Rearrangements," *Haematologica* 107, no. 1 (2022): 100–111.

45. C. R. Antonescu, L. Zhang, S. Y. Shao, et al., "Frequent *PLAG1* Gene Rearrangements in Skin and Soft Tissue Myoepithelioma With Ductal Differentiation," *Genes, Chromosomes & Cancer* 52, no. 7 (2013): 675–682.

46. G. Zhu, R. Benayed, C. Ho, et al., "Diagnosis of Known Sarcoma Fusions and Novel Fusion Partners by Targeted RNA Sequencing With Identification of a Recurrent *ACTB-FOSB* Fusion in Pseudomyogenic Hemangioendothelioma," *Modern Pathology* 32, no. 5 (2019): 609–620.

47. L. Song, Y. Zhang, Y. Wang, et al., "Detection of Various Fusion Genes by One-Step RT-PCR and the Association With Clinicopathological Features in 242 Cases of Soft Tissue Tumor," *Frontiers in Cell and Development Biology* 11 (2023): 1214262.

48. S. J. Logan, K. M. Schieffer, M. R. Conces, et al., "Novel Morphologic Findings in *PLAG1*-Rearranged Soft Tissue Tumors," *Genes, Chromosomes & Cancer* 60, no. 8 (2021): 577–585.

49. A. Tomás-Velázquez, L. F. Surrey, E. Miele, et al., "Mesenchymal *PLAG1* Tumor With *PCMTD1-PLAG1* Fusion in an Infant: A New Type of ″Plagoma″," *American Journal of Dermatopathology* 44, no. 1 (2022): 54–57.

50. M. L. Voz, N. S. Agten, W. J. Van de Ven, and K. Kas, "*PLAG1*, the Main Translocation Target in Pleomorphic Adenoma of the Salivary Glands, Is a Positive Regulator of *IGF-II*," *Cancer Research* 60, no. 1 (2000): 106–113.

51. M. L. Voz, J. Mathys, K. Hensen, et al., "Microarray Screening for Target Genes of the Proto-Oncogene *PLAG1*," *Oncogene* 23, no. 1 (2004): 179–191.

52. J. Declercq, F. Van Dyck, C. V. Braem, et al., "Salivary Gland Tumors in Transgenic Mice With Targeted *PLAG1* Proto-Oncogene Overexpression," *Cancer Research* 65, no. 11 (2005): 4544–4553.

53. X. Zhao, W. Ren, W. Yang, et al., "Wnt Pathway Is Involved in Pleomorphic Adenomas Induced by Overexpression of *PLAG1* in Transgenic Mice," *International Journal of Cancer* 118, no. 3 (2006): 643–648.

54. J. Declercq, I. Skaland, F. Van Dyck, et al., "Adenomyoepitheliomatous Lesions of the Mammary Glands in Transgenic Mice With Targeted *PLAG1* Overexpression," *International Journal of Cancer* 123, no. 7 (2008): 1593–1600.

55. J. Declercq, F. Van Dyck, B. Van Damme, and W. J. Van de Ven, "Upregulation of Igf and Wnt Signalling Associated Genes in Pleomorphic Adenomas of the Salivary Glands in *PLAG1* Transgenic Mice," *International Journal of Oncology* 32, no. 5 (2008): 1041–1047.

56. Y. Wang, W. Shang, X. Lei, et al., "Opposing Functions of *PLAG1* in Pleomorphic Adenoma: A Microarray Analysis of *PLAG1* Transgenic Mice," *Biotechnology Letters* 35, no. 9 (2013): 1377–1385.

57. M. Akhtar, C. Holmgren, A. Göndör, et al., "Cell Type and Context-Specific Function of PLAG1 for IGF2 P3 Promoter Activity," *International Journal of Oncology* 41, no. 6 (2012): 1959–1966.